RESEARCH ARTICLE

Temperature trends in Hawai'i: A century of change, 1917–2016

Marie M. McKenzie [iD] | Thomas W. Giambelluca | Henry F. Diaz

Department of Geography and Environment, University of Hawai'i at Mānoa, Honolulu, Hawaii

Correspondence
Marie M. McKenzie, Department of Geography and Environment, University of Hawai'i at Mānoa, 2424 Maile Way, Saunders Hall 445, Honolulu, HI 96822.
Email: mariemm@hawaii.edu

Funding information
University of Hawai'i at Hilo

Based on a revised and extended multi-station Hawai'i Temperature Index (HTI), the mean air temperature in the Hawaiian Islands has warmed significantly at 0.052°C/decade ($p < 0.01$) over the past 100 years (1917–2016). The year 2016 was the warmest year on record at 0.924°C above the 100-year mean (0.202°C). During each of the last four decades, mean state-wide positive air temperature anomalies were greater than those of any of the previous decades. Significant warming trends for the last 100 years are evident at low- (0.056°C/decade, $p < 0.001$) and high-elevations (0.047°C/decade, $p < 0.01$). Warming in Hawai'i is largely attributed to significant increases in minimum temperature (0.072°C/decade, $p < 0.001$) resulting in a corresponding downward trend in diurnal temperature range (−0.055°C/decade, $p < 0.001$) over the 100-year period. Significant positive correlations were found between HTI, the Pacific Decadal Oscillation, and the Multivariate ENSO Index, indicating that natural climate variability has a significant impact on temperature in Hawai'i. Analysis of surface air temperatures from NCEP/NCAR reanalysis data for the region of Hawai'i over the last 69 years (1948–2016) and a mean atmospheric layer temperature time series calculated from radiosonde-measured thickness (distance between constant pressure surfaces) data over the last 40 years (1977–2016) give results consistent with the HTI. Finally, we compare temperature trends for Hawaii's highest elevation station, Mauna Loa Observatory (3,397 m), to those on another mountainous subtropical island station in the Atlantic, Mt. Izaña Observatory (2,373 m), Tenerife, Canary Islands. Both stations sit above the local temperature inversion layer and have virtually identical significant warming trends of 0.19°C/decade ($p < 0.001$) between 1955 and 2016.

KEYWORDS
climate change, El Niño-southern oscillation, Hawai'i, Pacific decadal oscillation, radiosonde observations, temperature trends

1 | INTRODUCTION

The Pacific Ocean region plays an important role in ongoing global air and sea surface temperature changes. The Hawaiian Islands occupy a unique geographic position in the North-Central Pacific and possess a dense, long-term historical climate data record at a range of elevations spanning a mid-tropospheric temperature inversion produced by the descending arm of the Hadley cell. As such, Hawai'i is geographically well positioned to provide observations that enhance understanding of regional and global temperature trends, both at the surface and higher elevations in the atmosphere. In addition to yielding insights for regional and global climate, temperature change in the Hawaiian archipelago can have critically important impacts on terrestrial ecosystems, water supply, agriculture, and economic health (Keener *et al.,* 2012).

The Hawaiian temperature record also provides an opportunity to examine the effects of large sources of internal climate variability—the El Niño–Southern Oscillation (ENSO) and the Pacific Decadal Oscillation (PDO; Mantua *et al.,* 1997). Hawai'i is close to the centres of action of

ENSO, the strongest driver of natural global climate variability on time scales of two to seven years (Salinger, 2005). Whether PDO is a dynamic mode of climate variability independent of ENSO has been questioned (Schneider and Cornuelle, 2005). Nevertheless, the PDO Index (Zhang et al., 1997; Mantua and Hare, 2002) provides a convenient metric for basin-wide climate variation at the decadal scale, while an ENSO index such as the Multivariate ENSO Index (MEI) provides a statistic representing interannual variations. PDO phase changes have been associated with oceanic circulation changes linked to variations in the rate of global temperature increase, including the recently ended period of slow global warming (Dai *et al.,* 2015).

In support of a state-wide surface air temperature analysis, Giambelluca *et al.* (2008) ; hereafter referred to as GDL, developed the Hawai'i Temperature Index (HTI) to evaluate mean (T_{mean}), minimum (T_{min}), and maximum (T_{max}) temperature trends in the islands. Observations from 21 stations across five of the main Hawaiian Islands were included in the index, calculated as the mean of monthly station anomalies, averaged to annual values. GDL showed increases in T_{mean}, T_{min}, and T_{max} at rates of 0.043, 0.094, and 0.005°C/decade state-wide, respectively, over the 88-year period, 1919–2006. The more rapidly rising T_{min} and the consequent reduction in the diurnal temperature range (DTR) were key findings of GDL. In the more recent decades of their study (1975–2006), mean warming rates were much steeper state-wide (0.164°C/decade), approaching the global mean trend of 0.177°C/decade (1976–2005; Pachauri *et al.,* 2014), with enhanced warming at high-elevation stations (0.268°C/decade). Mountain temperatures in Hawai'i vary over short distances due to factors, such as the vertical structure of the atmosphere and the interaction of winds with the topography of the islands. GDL found positive temperature trends, at both low- and high-elevations, comparable to changes observed in other tropical and subtropical oceanic islands (Huber *et al.,* 2006; Martín *et al.,* 2012; Diaz *et al.,* 2014), and examined fluctuations in the rate of warming over the 1919–2006 period. While previous work has linked ENSO- and PDO-related natural variability with fluctuations in temperature (Giambelluca *et al.,* 2008 ; Diaz *et al.,* 2011) and precipitation (Diaz and Giambelluca, 2012; Frazier *et al.,* 2018) in Hawai'i, apparent shifts in these teleconnections are not well understood. GDL noted, for example, that in the most recent decades of their study, temperature appeared to be less sensitive to phase changes in the PDO.

With GDL as the starting point for this analysis, we sought to extend the 88-year HTI record to 100 years. The original HTI network of 21 stations actually had available between 8 and 18 stations in any given year, and the number of stations in the index had declined steadily from its peak in the 1950s due to station closings. With further declines in recent years, the homogeneity of the HTI, based on its

changing network, became questionable. Hence, it is necessary to re-evaluate and refine the index to address problems associated with the network. To do so, we develop a new HTI by merging temperature anomaly time series from two networks, spanning the early and late portions of the 100-year study period, respectively. Extending the time series even by a few years is significant because the addition of recent years captures both the period of a widely observed global warming slowdown, which has been linked to PDO-related changes in Pacific Ocean circulation patterns (Dai *et al.,* 2015), and the 2015–2016 El Niño, ranked among the three strongest El Niño events in the historical record (L'Heureux *et al.,* 2017). Including these events in the time series adds significantly to the available information on regional temperature effects of ENSO and PDO.

To further expand on the work of GDL, in this study, we have conducted additional analyses to validate the HTI trends, by comparing the station-based index with time series derived from NCEP/NCAR reanalysis data and a mean atmospheric layer temperature time series derived from the difference in geopotential height observations at two pressure levels. We also re-examined the GDL conclusions on the difference in warming trends between low- and high-elevations in Hawai'i, considering possible spurious effects of small sample size and data gaps. Finally, in light of the phenomenon of enhanced warming with elevation more generally (Pepin *et al.,* 2015), we examine temperature trends for the highest elevation station in the islands, Mauna Loa Observatory (19.54° N, 155.58° W, 3397 m), and compared results with that of a high-elevation subtropical island station in the Atlantic, Mt. Izaña Observatory (28.30° N, 16.50° W, 2373 m), Tenerife, Canary Islands. Both of these stations are located above the local trade wind inversion level and, hence, subject to effects of changes in Hadley cell circulation. The similarity of long-term temperature trends in the Canary Islands, as shown by Martín *et al.* (2012), to those previously found for Hawai'i led us to compare temperature changes, particularly at higher elevations, at these two widely separated, but similarly situated sites.

2 | METHODS

GDL used a temperature index (1919–2006) derived from 21 stations (Table 1) distributed across the main Hawaiian Islands. In this analysis, we added 12 additional years of data from the National Oceanographic and Atmospheric Administration's (NOAA's) National Centers for Environmental Information (NCEI, http://www.ncdc.noaa.gov/cdo-web/) and the Western Regional Climate Center (WRCC, https://wrcc.dri.edu/summary/Climsmhi.html) from 1917–1918 and 2007–2016 to the GDL HTI time series. Monthly T_{mean}, T_{min}, and T_{max} surface air temperature (SAT) are analysed, and station annual temperature anomalies were calculated as the mean of the monthly anomalies in each year. Stations missing more

TABLE 1 Locations and elevations for the 21 climate stations used in the study by Giambelluca *et al.* (2008) and the 14 of which (marked) were used in this study

SKN	Station name	Status	Elevation (m)	Latitude (°N)	Longitude (°W)
39	Mauna Loa Slope Observatory[a]	1955 to present	3,341	19.54	155.58
338	Haleakalā Ranger Station[a]	1939 to present	2,143	20.76	156.25
54	Hawai'i Volcanoes Nat'l Park HQ[a,b]	1949–2014	1,211	19.43	155.26
267	Kula Sanatorium/Hospital[a,b]	1916 to present	916	20.70	156.36
436	Ka'ili'ili	1925–2012	744	20.51	156.16
434	Haleakalā BES/Farm Exp 4	1939–1992	640	20.51	156.18
672	Lāna'i City	1930–2014	494	20.50	156.55
91	Mountain View	1906–1985	466	19.33	155.07
714	Tantalus	1936–1957	427	21.21	157.49
446	Kailua[b]	1905 to present	213	20.89	156.22
73.2	Kainaliu	1939–2013	457	19.54	155.93
870	'Ōpae'ula[b]	1949 to present	288	21.57	158.04
21	Pāhala[b]	1905–1985	264	19.12	155.29
175.1	Kohala Mission[b]	1905–1978	164	20.14	155.48
223	'Ō'ōkala[b]	1949–1993	131	20.10	155.17
1,020	Līhu'e[b]	1905–1963	63	21.59	159.22
781	Kāne'ohe Mauka	1928–1998	60	21.25	157.49
1,020.1	Līhu'e Airport[a]	1950 to present	30	21.98	159.34
86	Hilo[a,b]	1905 to 1966	12	19.44	155.05
87	Hilo Airport[a,b]	1941 to present	12	19.72	155.06
703	Honolulu WB Airport[a]	1946 to present	2	21.32	157.93

SKN: state key number used to identify climate stations.
[a]Included in the 8-station network.
[b]Included in the 10-station network.

than one monthly value in a given year were excluded. Monthly anomalies were calculated as departures from the baseline period (1944–1980) mean monthly values at each station. The baseline period corresponds to the period with the greatest number of index stations available. For each station, the annual temperature anomaly time series was calculated as the departure relative to the station annual mean over the baseline period. To address outliers, any values outside of the 99% confidence interval (set as ±2.326 standard deviations derived from a running 31-year sample), were excluded from the analysis. Following GDL, temperature indices were computed separately for state-wide, low- (below 800 m), and high-elevation stations (above 800 m). Because of the scarcity of high-elevation stations, the limit was set in GDL at 800 m to include four stations, and retained here for the same reason. The HTI anomalies were calculated as the weighted mean of the low- and high-elevation indices with weights of 0.575 and 0.425 corresponding to the relative proportion of land area below and above 800 m elevation, respectively.

Due to the various establishment and discontinuation dates of stations (Table 1) the use of a single GDL network for this extended analysis would have led to increasingly greater effects of changes in network membership over time (Figure 1a). Homogeneity is questionable if the number of stations in the index changes significantly over the period under study. Therefore, we re-evaluated the reference network for this study. Many long-term stations were available early in the period but discontinued in the middle of the study period, while other stations started in the middle and continued toward the end of the period. To address this problem, while trying to maximize the spatial coverage throughout the period, we established two networks to represent the early and late parts of the record (Figure 1b, c). The time series of the early and late networks were merged with a total of 14 stations (Figure 2), four of which were common to the two networks (Table 1), after adjustment of the earlier network index that is based on a linear regression between the two networks during the period of overlap (1952–1983) to achieve a homogeneous 100-year index time series. This process was done separately for T_{mean}, T_{min}, and T_{max} time series, state-wide, and for low- and high-elevation stations. Subsequently, the F-ratio test was used to assess the significance of the difference in the variances between the regression-adjusted temperature time series of the earlier period and that of the original time series of the later period.

As a measure of temperature variation in the broader region, mean SAT, and mean sea surface temperatures (SST) based on NCEP/NCAR reanalysis data (Kistler *et al.*, 2001; NCEP reanalysis data provided by the NOAA/OAR/ESRL PSD, Boulder, Colorado, USA, from their website at http://www.esrl.noaa.gov/psd/) were analysed. We also examined
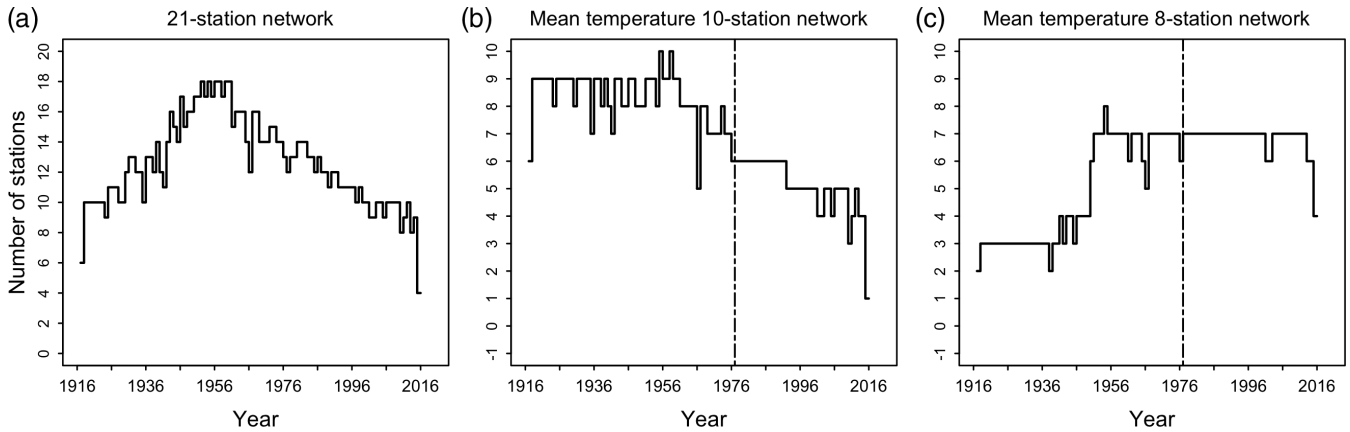
FIGURE 1 (a) Number of stations available in the 21-station network (GDL) during 1917–2016, (b) total number of stations in each year for the early 10-station subset network, and (c) total number of stations in each year for the later 8-station subset network. Vertical dashed line indicates the period (1977) where the two networks were merged
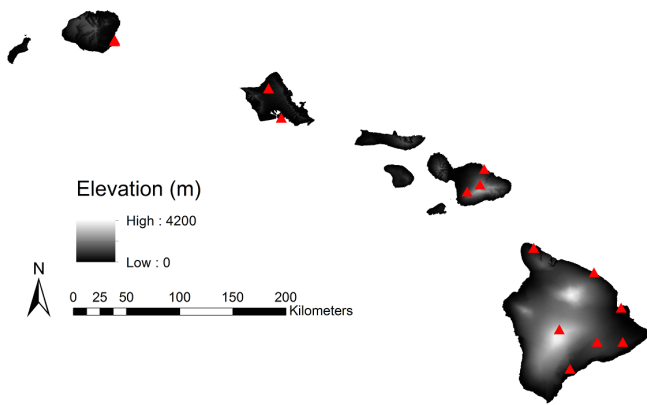

FIGURE 2 Elevation map of the temperature stations (red triangles) across the Hawaiian islands used in this study [Colour figure can be viewed at wileyonlinelibrary.com]

the NOAA Extended Reconstructed Sea Surface Temperature v5 dataset provided by the NOAA/OAR/ESRL PSD, Boulder, Colorado, USA, from their website at https://www.esrl.noaa.gov/psd (ERSST v5, Huang *et al.,* 2017) around Hawai'i for comparison with the HTI results. The datasets were obtained for the HTI period (1917–2016).

The multivariate ENSO Index (MEI; Wolter and Timlin, 1998) was used to represent ENSO status in this study. The MEI includes six observed fields (SLP, zonal and meridional surface wind, SST, and total cloudiness) in the classification of ENSO modes. MEI data were obtained from NOAA (http://www.esrl.noaa.gov/psd/enso/mei/table.html). PDO index values were obtained for the HTI period of record from the Joint Institution for the Study of the Atmosphere and Ocean (http://research.jisao.washington.edu/pdo/PDO.latest.txt).

Toumi *et al.* (1999) showed that observed pressure variations at high-elevation could be used to estimate temperature change in the underlying air layer. Here, we followed a similar approach and analysed the difference in geopotential height observations at two pressure levels (700 and 1,000 hPa) from Hawaiian radiosonde data to derive the time series of mean 1,000–700 hPa (approximately the

lowest 3,000 m) air layer temperature (MLT). The MLT time series (1977–2016) was calculated as a function of the geopotential height difference or layer thickness based on the assumption of the hydrostatic equilibrium:

$$\frac{dp}{dz} = -\rho g, \tag{1}$$

where dp/dz is the vertical pressure gradient, ρ is air density, and g is acceleration due to gravity 9.81 m s^{-2}. Applying this relationship to a specific layer and substituting for ρ using the equation of state ($\rho = \frac{p}{R_d T_v}$, where R_d is the gas constant for dry air, 287 J kg^{-1} K^{-1}, and $\bar{T}_v$ is the mean *virtual* temperature of the air layer) results in (Wallace and Hobbs, 1977):

$$z_2 - z_1 \frac{R_d \bar{T}_v}{g} \ln\left(\frac{p_1}{p_2}\right) \tag{2}$$

where z_1 and z_2 are the geopotential heights (m) corresponding to pressure levels p_1, and p_2 (hPa). Rearranging, $\bar{T}_v$ is obtained as:

$$\bar{T}_v = \frac{(z_2 - z_1)}{\frac{R_d}{g} \ln\left(\frac{p_1}{p_2}\right)} \tag{3}$$

This equation was applied using height observations at the 1,000 hPa (~150 m a.s.l.) and 700 hPa (~3,200 m a.s.l.) levels measured twice daily 0:00 UTC (2:00 p.m. HST) and 12:00 UTC (2:00 a.m. HST) from an atmospheric sounding station at Hilo (19.72°N, 155.05°W) on Hawai'i Island (http://weather.uwyo.edu/upperair/sounding.html).

Statistical analyses were performed in the R statistical programming environment (R core Team, 2014). Secular trends were calculated through linear regression using the gls function in the *nlme* package (Pinheiro *et al.,* 2017) to explicitly account for temporal autocorrelation and fitted the regression equation using restricted maximum likelihood (REML). We assessed statistical significance at levels of 0.001, 0.01, and 0.05, for the null hypothesis that the trend is zero. In addition to the secular trend analyses, the
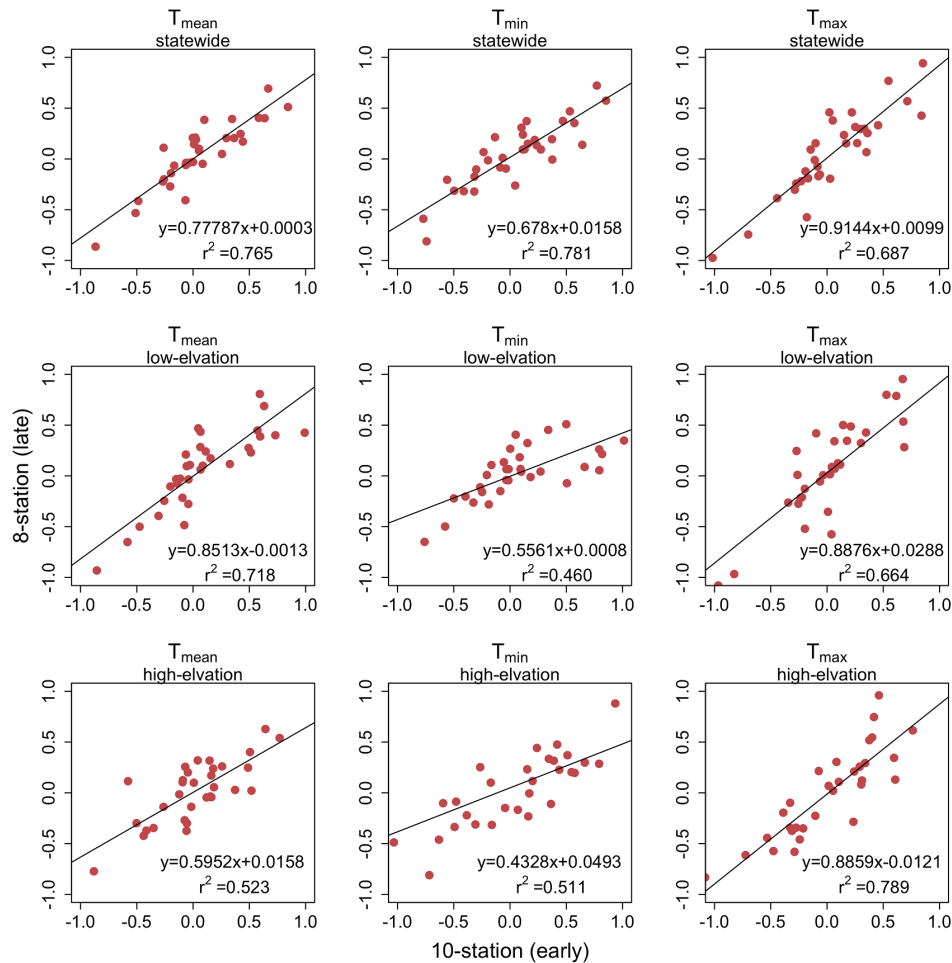
FIGURE 3 Linear regression plots for annual mean temperature anomaly time series for the 10-station (x variable) and 8-station (y variable) networks during the overlap period (1952–1983). The 10-station time series were subsequently adjusted using the linear regression equations shown here [Colour figure can be viewed at wileyonlinelibrary.com]

Pearson product–moment correlation coefficients were computed for assessing the relationships between atmospheric variables and temperature indices.

3 | RESULTS

3.1 | Network testing

Two temperature subset station networks were evaluated to represent the early and late parts of the study period. A 10-station network was selected with nearly continuously available data at all stations during 1917–1983. Similarly, an eight-station network was identified with nearly complete data during 1952–2016. Data from these network stations were screened, and anomalies outside of the 99th percentile were removed from the analysis. For each of T_{mean}, T_{min}, and T_{max} and for state-wide, low- and high-elevation stations, linear regressions between the annual time series of the two networks during the overlapping period, 1952–1983, were performed (Figure 3). Results from the linear regressions showed good relationships and were used to adjust the early time series to correct for any systematic heterogeneity arising from merging the two records. The state-wide mean bias errors (MBE) between the two time series for T_{mean}, T_{min}, and T_{max} during the 1952–1983 period before the adjustments were 0.012, −0.001, and − 0.005°C, respectively. After the adjustments, state-wide MBE values were reduced to −0.007, −0.000001, and 0.00003°C, respectively, for T_{mean}, T_{min}, and T_{max} (see Table 2 for MBE values for all time series before and after adjustments). The F-ratio test was used to compare the variances of the time series derived from the two networks during the overlapping period after the adjustments and found no statistically significant differences. Therefore, for state-

TABLE 2 Mean bias error (MBE) values (°C) for all time series during overlapping periods of the earlier (10-station) and original later (8-station) networks before and after linear regression adjustments

	Annual series	T_{mean}	T_{min}	T_{max}
State-wide	Before adjustment	0.01180	−0.00114	−0.00497
	After adjustment	−0.00692	−0.0000014	0.00003
Low-elevation	Before adjustment	0.01238	0.03379	−0.02158
	After adjustment	0.00002	−0.00002	−0.00002
High-elevation	Before adjustment	−0.00748	−0.00002	0.01750
	After adjustment	−0.00003	−0.04841	−0.0000098

wide, low-, and high-elevation stations, the two time series were merged at the end of 1977, approximately in the middle of the period of overlap, to create 100-year time series of T_{mean}, T_{min}, and T_{max}. The new HTI (T_{mean}, T_{min}, and T_{max} for state-wide, low- and high-elevation stations) have strong relationships with the previously defined HTI of GDL (Figure 4). The new anomaly time series for state-wide T_{mean}, T_{min}, and T_{max} temperatures were tested against the corresponding GDL time series, yielding coefficients of determination (r^2) of 0.92, 0.94 and 0.87, respectively.

3.2 | Station surface air temperature trends

The trends in near-surface temperature for state-wide (Figure 5) and both low- and high- elevations stations (Figure 6) are summarized in Table 3. Based on the long-term (1917–2016) data, including the additional 12 years included in this analysis, Hawaii's 100-year T_{mean} has a statistically significant positive trend of 0.052°C/decade ($p < 0.01$; Figure 5a). As demonstrated in GDL, warming is largely attributed to an increase in T_{min}, which has seen a significant long-term warming trend of 0.072°C/decade

($p < 0.001$) state-wide (Figure 5b). T_{max} (Figure 5c), on the other hand, was found to have no significant long-term trend. The increase in T_{min} and the consistency in T_{max} imply a significant reduction in DTR over the long-term period (Figure 5d) with a trend of −0.054°C/decade ($p < 0.001$).

T_{mean} at low-elevation stations over the 100-year period (1917–2016) shows a positive trend of 0.056°C/decade ($p < 0.001$; Figure 6a). At high-elevation stations, T_{mean} over the long-term period was found to have a significant positive trend of 0.047°C/decade ($p < 0.01$; Figure 6b). A significant rate of warming for T_{min} (0.090°C/decade; $p < 0.001$) is also found at low-elevation stations (Figure 6c). T_{min} at high-elevation stations did not show a significant trend over the long-term (Figure 6d). T_{max}, for both low- and high-elevation stations, shows no significant trend between 1917 and 2016 (Figure 7e–f).

Trends during subsets of the 100-year study period, defined according to apparent periods of warming (+) and cooling (−), 1917–1939 (+), 1940–1957 (−), 1958–1999 (+), and 2000–2013 (−), are also summarized in Table 3. While temperature has fluctuated over the past 100 years, the long-term trend is clearly upward. Although the period
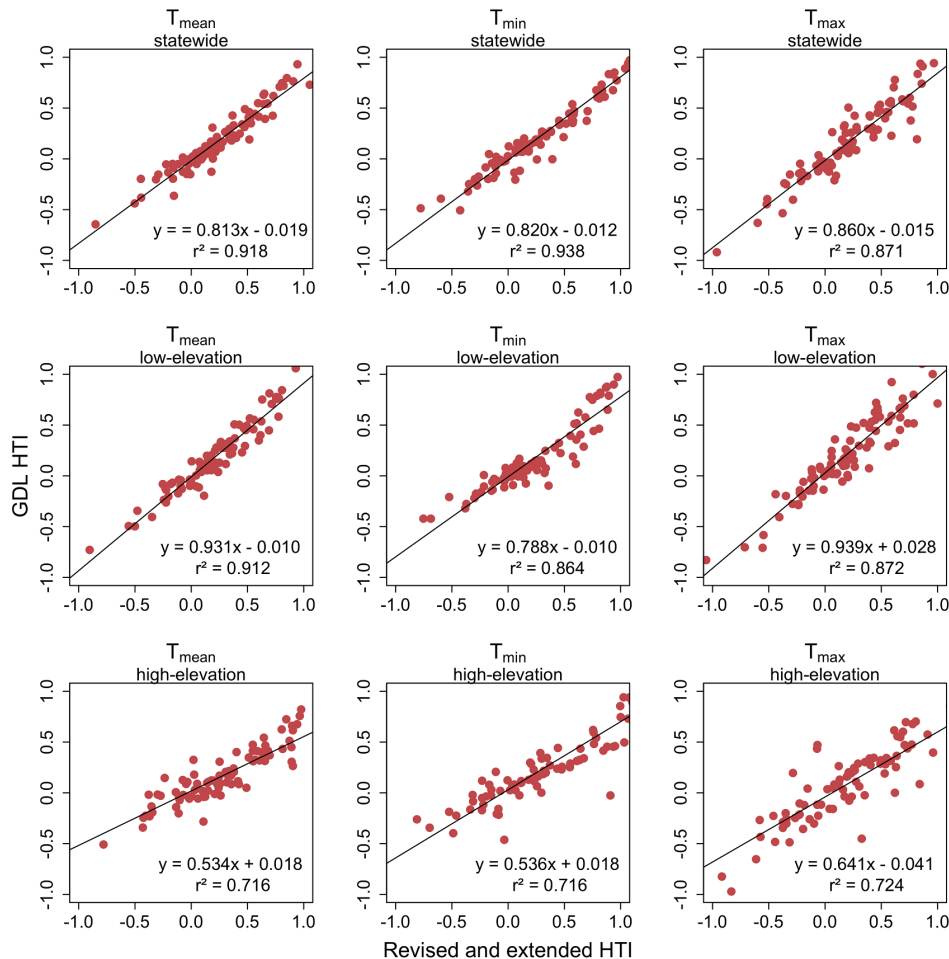

FIGURE 4 Comparison of annual mean temperature anomalies used in the GDL HTI (*y* variable) and the revised and extended index presented in this study (*x* variable) from 1919 to 2006, which have good to strong relationships [Colour figure can be viewed at wileyonlinelibrary.com]
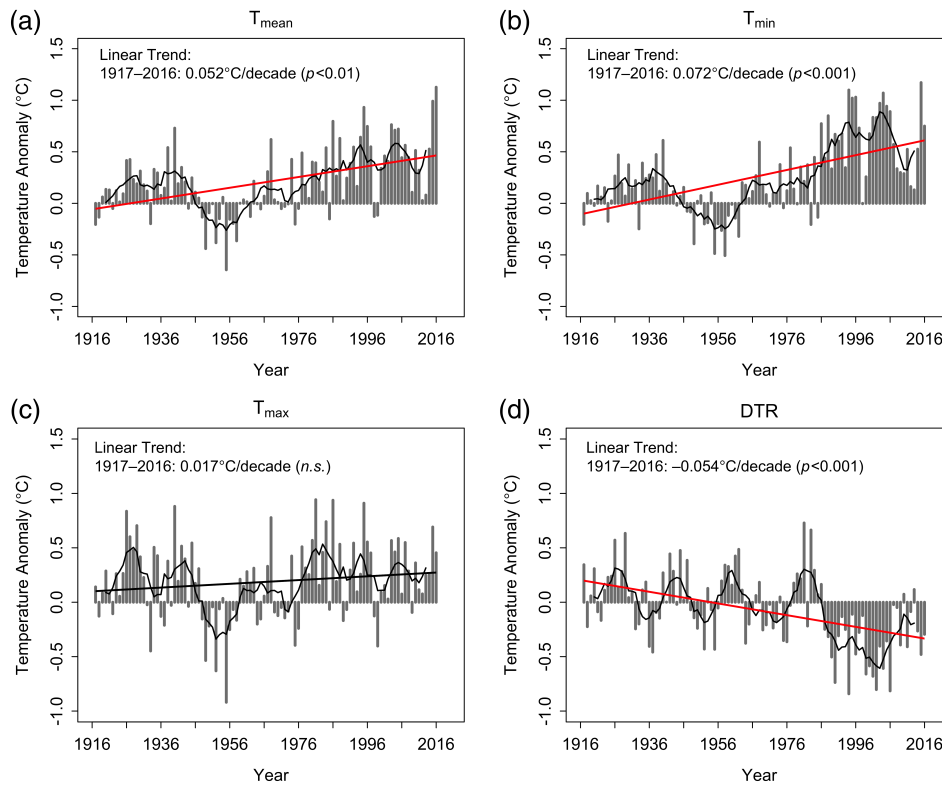
FIGURE 5 Temperature anomalies for HTI in Hawai'i are shown as the annual mean relative to 1944–1980, with individual years shown as grey bars. The black curve represents the 7-year running mean, and the lines correspond to the linear regressions for the 100-year period (1917–2016). The red lines indicate significant trends. Non-significant trend is marked n.s. ($p > 0.05$) [Colour figure can be viewed at wileyonlinelibrary.com]

2000–2013 had no significant changes in T_{mean}, T_{min}, or T_{max} state-wide, the last 3 years of the analysis, with 2015 and 2016 being the warmest years on record, strongly suggest that rapid warming has resumed. The years 2014–2016 were exceptionally warm. However, even with 2015–2016 removed from the time series, the long-term (1917–2014) trends in T_{mean} (0.042°C/decade; $p < 0.01$) and T_{min} (0.066°C/decade; $p < 0.001$) remain significant.

During the last four decades, state-wide decadal mean T_{mean} and T_{min} anomalies were all higher than those of any of the previous decades (Table 4). A particularly interesting feature is the accelerated rate of increase in the last few decades for T_{min} state-wide and at low-elevation stations. At both low- and high-elevation stations, T_{mean} and T_{min} in the three most recent decades (excluding the recent decade for high-elevation stations) were higher than in all previous decades. Decadal means for T_{max}, on the other hand, have stabilized since 1987.

To assess the effect of adjusting the time series based on the 10-station network (representing the earlier part of the study period), trends were also calculated from the unadjusted time series. Long-term trends for the merged time series without adjustments (for T_{mean}, T_{min}, and T_{max}, temperatures state-wide and at both elevation ranges) are slightly lower than the long-term trends derived from the regression-adjusted time series, excluding the long-term trend at low-elevation, which remains the same (Table 5).

3.3 | Temperature trends derived from other data sets

An alternative regional temperature time series was derived using NCEP/NCAR reanalysis data (Kistler *et al.,* 2001) for comparison with our HTI results. Annual SATs over the Hawai'i region, 15–25°N, 170–140°W, was analysed during 1948–2016. While not entirely independent of the station data, the mean of gridded estimates for the region provide a metric of the broader regional temperature variation with assimilation of all available observations. The resulting temperature time series (Figure 7) has a positive trend of 0.103°C/decade ($p < 0.01$) over this 69-year period, similar to the positive HTI trend for the same period (0.122°C/decade; $p < 0.001$). The two time series are also well correlated (r = 0.84; $p < 0.001$).

Geopotential height observations for the period 1977–2016 from radiosonde data provided an additional temperature estimate for comparison with the HTI results. The 700–1,000 hPa atmospheric MLT corresponds well with the state-wide HTI over this period (Figure 8). While the correlation between the two temperature estimates is reasonably high (r = 0.64, $p < 0.001$), neither time series had a significant trend over the 40-year overlap period. MLT has a non-significant negative trend of −0.015°C/decade. Please note that estimation based on the geopotential height difference gives virtual temperature of the air layer between 1,000 and 700 hPa ($\bar{T}_v$), which can be affected by changes in specific humidity within the layer over time. Diaz *et al.* (2011)
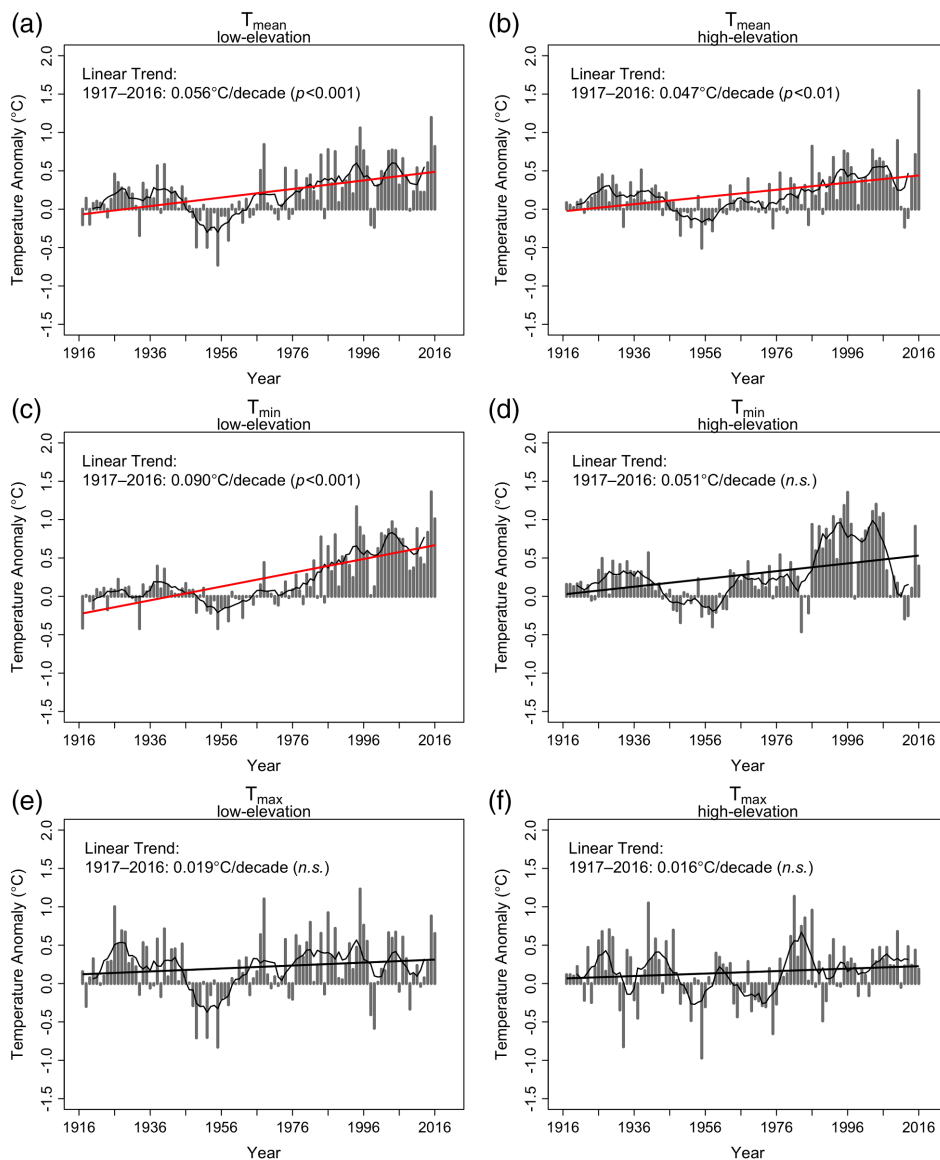
FIGURE 6 Temperature anomalies for HTI in Hawai'i for low-elevations (left column; (a), (c), and (e) and high-elevations (right column; (b), (d), and (f) shown as the annual anomaly relative to 1944–1980, with individual years shown as grey bars. The black curve represents the 7-year running mean, and the lines correspond to linear regressions for the 100-year period (1917–2016). The red lines indicate significant trends. Non-significant trends are marked n.s. ($p > 0.05$) [Colour figure can be viewed at wileyonlinelibrary.com]

showed that specific humidity in the 1,000–700 hPa layer increased by about 0.15 g kg^{-1} during 1958–2009. Assuming the specific humidity increased during 1977–2016 at the same rate as during 1958–2009, the humidity change would have accounted for an increase in $\bar{T}_v$ of about 0.02°C (Elliott *et al.,* 1994, Equation 3).

The HTI time series is compared with the two large-scale modes of natural internal climate variability, PDO and ENSO, for the 100-year study period (1917–2016) in Figure 9. HTI has a reasonably strong relationship with PDO (Figure 9a) ($r = 0.53$, $p < 0.001$), whereas the HTI and MEI (Figure 9b) have a weaker, but significant positive correlation ($r = 0.34$, $p < 0.001$). GDL and Diaz *et al.* (2011) showed that Hawai'i temperature variations are strongly coupled to the PDO and SST, but that in recent decades air temperature in Hawai'i had increased relative to the

variations in the PDO index. After revising and extending the HTI time series, temperature still appears to be rising relative to the variations driven by the PDO (Figure 9a). Comparing recent HTI time series with NCEP/NCAR SST anomalies averaged over 16–24°N and 160–140°W for the period 1948–2016 (Figure 10a) shows that while air temperature in the islands is positively correlated with SST of the surrounding area ($r = 0.53$; $p < 0.001$), the SST trend of 0.032°C/decade is much lower that the HTI trend, 0.122°C/decade, for the same period. We also compared HTI with another SST data set available for a longer period, NOAA ERSST v5, averaged over 15–30°N and 170–140°W. Over the whole study period (1917–2016), it also showed a positive correlation ($r = 0.65$; $p < 0.001$; Figure 10b), and, in this case, a trend very similar to the HTI trend (ERSST: 0.056°C/decade vs. HTI: 0.052°C/decade).

TABLE 3 Linear air temperatures trends for elevation ranges in Hawai'i and the whole state, for the entire period of record and for the periods with apparent warming and cooling

	Annual series	T_{mean} (°C/decade)	T_{min} (°C/decade)	T_{max} (°C/decade)	DTR (°C/decade)
State-wide	1917–2016	0.052**	0.072***	0.017	−0.054***
	1917–1939	0.115	0.137*	0.025	−0.161
	1940–1957	−0.428***	−0.323***	−0.589***	−0.264*
	1958–1999	0.119**	0.197***	0.059	−0.144*
	2000–2013	−0.271	−0.420	−0.053	0.560***
Low-elevation	1917–2016	0.056***	0.090***	0.019	
	1917–1939	0.102	0.117	0.020	
	1940–1957	−0.410***	−0.256***	−0.541**	
	1958–1999	0.120*	0.177***	0.053	
	2000–2013	−0.217	−0.252	−0.196	
High-elevation	1917–2016	0.047**	0.051	0.016	
	1917–1939	0.073	0.085	−0.081	
	1940–1957	−0.266**	−0.264 *	−0.610 ***	
	1958–1999	0.120***	0.220**	0.060	
	2000–2013	−0.387	−0.768	0.059	

Symbols following fitted coefficient indicate statistical significance level at alpha: ***0.001; **0.01; *0.05; other values not significant.
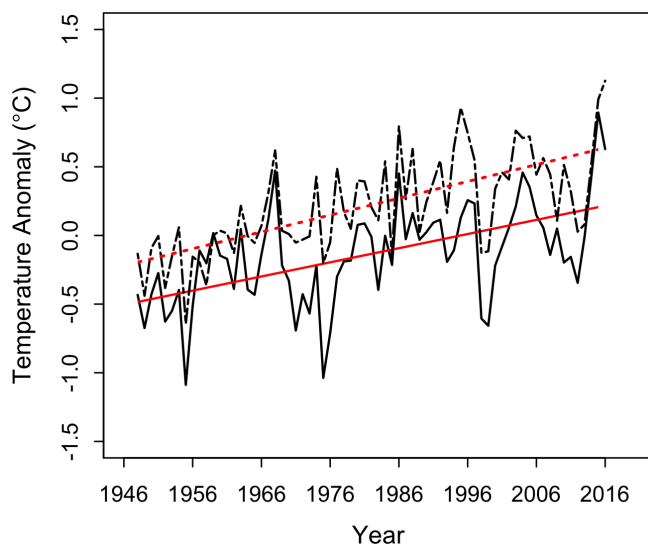

FIGURE 7 Mean annual SAT anomalies from NCEP/NCAR reanalysis data (black solid line) for Hawai'i region (15–25°N, 170–140°W) from 1948 to 2016 compared to the HTI (black dotted line). Linear trend for NCEP/NCAR reanalysis data temperature is 0.103°C/decade (red solid line) and the HTI trend is 0.122°C/decade (red dotted line) over the 69-year period, 1948–2016 (both significant, $p < 0.001$.). There is a strong correlation between two the data sets ($r = 0.84$; $p < 0.001$) [Colour figure can be viewed at wileyonlinelibrary.com]

In comparison with either of the SST data sets, HTI increases faster than SST starting around 1950, as was also noted by GDL. It remains unclear why air temperature and SST have similar centennial scale trends, but apparently differ on shorter time scales. Possible explanations include climate variations that affect land areas differently than the surrounding ocean areas (affecting for example night time cloud cover over the islands), and land cover changes. We note that irrigated sugarcane acreage expanded rapidly

before around 1940 (Juvik and Juvik, 1998, p. 246), which might have suppressed the air temperature trend relative to the SST trend during that time. Hawaii's urbanized area has experienced rapid expansion since the time of statehood (1959) coincident with a decline in irrigated sugarcane, perhaps contributing to enhanced air temperature warming relative to SST since that time.

Of particular interest is the apparent tuning of the Hawai'i air temperature time series to the global warming signal. The long-term (1917–2016) global land-ocean temperature index (GLOTI) in Figure 11a and the global ocean-only temperature index (GOTI) in Figure 11b time series (NOAA/NCEI, 2017; http://www.ncdc.noaa.gov/cag/) have somewhat stronger warming trends than Hawaii's at 0.098°C/decade and 0.081°C/decade, respectively. The 20-year running trends are determined and compared between the HTI, GLOTI, GOTI, and lowess-smoothed PDO time series in Figure 11. Prior to around 1970, Hawaii's temperature responses to natural climate variability appear to have been more pronounced than those of the global indices. Following 1970, however, HTI tracks GLOTI and GOTI closely, lending confidence to the apparent link between regional and global warming.

Figure 12 shows mean surface temperature from Mt. Izaña Observatory (2,373 m), Tenerife, Canary Islands (source of data: Emilio Cuevas, AEMET, Canary Islands, Spain) for comparison with Mauna Loa Observatory (MLO) in Hawai'i, elevation 3,397 m. Mt. Izaña, shown in Figure 12a, has a significant positive T_{mean} of 0.15°C/decade ($p < 0.001$) over 1917–2016, and 0.19°C/decade ($p < 0.001$) for the 62-year period (1955–2016). MLO, in Figure 12b, also has a mean warming trend of 0.19°C/decade ($p < 0.001$) for the 62-year period

TABLE 4 Decadal mean surface mean, minimum, and maximum temperature anomalies (°C) 1917–2016 state-wide and for high and low elevation stations

	Annual series	T_{mean}	T_{min}	T_{max}
State-wide	1917–1926	0.058	0.040	0.178
	1927–1936	0.197	0.213	0.276
	1937–1946	0.250	0.203	0.281
	1947–1956	−0.189	−0.143	−0.247
	1957–1966	−0.041	−0.082	0.059
	1967–1976	0.106	0.172	0.041
	1977–1986	0.300	0.249	0.482
	1987–1996	0.458	0.707	0.314
	1997–2006	0.415	0.720	0.189
	2007–2016	0.470	0.476	0.295
Low-elevation	1917–1926	0.055	−0.037	0.201
	1927–1936	0.174	0.032	0.349
	1937–1946	0.231	0.153	0.278
	1947–1956	−0.225	−0.095	−0.309
	1957–1966	−0.052	−0.084	0.046
	1967–1976	0.169	0.078	0.214
	1977–1986	0.345	0.246	0.449
	1987–1996	0.510	0.579	0.461
	1997–2006	0.400	0.641	0.176
	2007–2016	0.491	0.704	0.281
High-elevation	1917–1926	0.116	0.125	0.138
	1927–1936	0.206	0.313	0.162
	1937–1946	0.195	0.170	0.268
	1947–1956	−0.122	−0.088	−0.142
	1957–1966	0.008	−0.008	0.076
	1967–1976	0.063	0.204	−0.192
	1977–1986	0.233	0.219	0.522
	1987–1996	0.388	0.880	0.116
	1997–2006	0.475	0.826	0.207
	2007–2016	0.442	0.167	0.314

(1955–2016). MLO and Mt. Izaña's temperatures anomalies are plotted together in Figure 12c to show the similarities and are significantly correlated with each other ($r = 0.51$, $p < 0.001$; Figure 12d).

4 | DISCUSSION

The result presented here of a mean long-term period (1917–2016) warming rate for Hawai'i of 0.052°C/decade ($p < 0.01$) updates the previously analysed temperature change in Hawai'i for 1919–2006 (GDL; 0.043°C/decade, $p = 0.05$). The warming trend in Hawai'i amounts to more than half the global rate over the past century of 0.098°C/decade (NOAA/NCEI, 2017). HTI time series and the GLOTI time series show substantial coherency in the timing of periods of accelerated and reduced warming (Figure 11a).

GDL found that the rate of warming was much greater at high-elevations than low-elevations during 1975–2006. Their finding is consistent with expectations and observations of amplified warming with elevation (Pepin et al., 2015). Diaz et al. (2011) analysed free atmosphere temperature trends along the vertical profile over Hawai'i using NCEP reanalysis data. They found warming throughout the profile with a distinct peak at the 850 hPa level, which differs from the station-based findings of GDL. The extended HTI analysis shows (see Table 3) that T_{mean} at low-elevation stations has a significant warming trend of 0.056°C/decade ($p < 0.001$) compared to 0.043°C/decade in the GDL series. At high-elevation stations ($n = 4$), T_{mean} over 1917–2016 increased at 0.047°C/decade ($p < 0.01$), slightly higher than for the 85-year study period analysed by GDL (0.044°C/decade, $p = 0.05$), but lower than the low-

TABLE 5 Surface temperature trend anomalies for merged time series without linear regression-adjustments for 1917–2016 state-wide, and for high- and low-elevation stations

	Annual series	T_{mean} (°C/decade)	T_{min} (°C/decade)	T_{max} (°C/decade)	DTR (°C/decade)
State-wide	1917–2016	0.046**	0.067**	0.016	−0.050**
	1917–1939	0.145	0.202*	−0.027	−0.225
	1940–1957	−0.580***	−0.476***	−0.644***	−0.161
	1958–1999	0.114**	0.205***	0.060	−0.160*
	2000–2013	−0.272	−0.419	0.053	0.560***
Low-elevation	1917–2016	0.032	0.090***	0.021	
	1917–1939	0.120	0.211	0.023	
	1940–1957	−0.481***	−0.461***	−0.610**	
	1958–1999	0.118*	0.184***	0.060	
	2000–2013	−0.217	−0.252	−0.196	
High-elevation	1917–2016	0.038	0.033	0.011	
	1917–1939	0.123	0.200	−0.091	
	1940–1957	−0.446**	−0.611*	−0.688***	
	1958–1999	0.118***	0.242**	0.054	
	2000–2013	−0.388	−0.768	0.150	

Symbols following fitted coefficient indicate statistical significance level at alpha: ***0.001; **0.01; *0.05; other values are not significant.
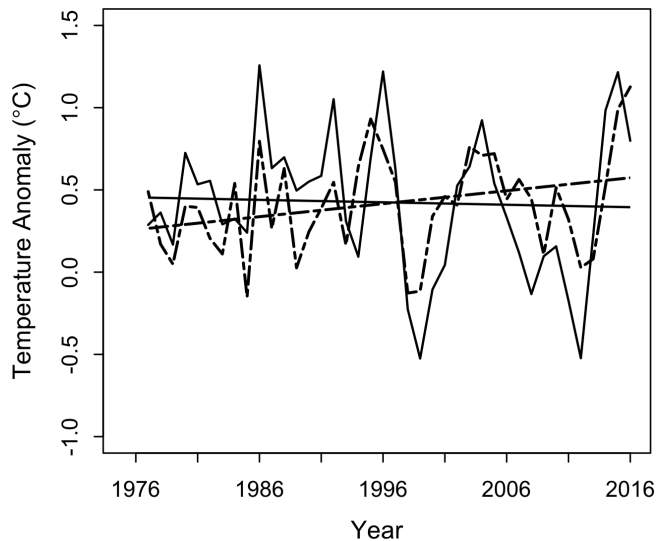
FIGURE 8 Mean atmospheric layer temperature (MLT) anomalies from Hilo radiosonde height (m) between the 1,000 and 700 hPa surfaces relative to 1985–2005 base period and mean surface temperature anomalies in Hawai'i (HTI). Linear trend for MLT (——) is −0.015°C/decade over the 40-year period, 1977–2016 (not significant; $p = 0.90$) and the linear trend for temperature (------) is 0.079°C/decade over the 40-year period, 1977–2016 (not significant; $p = 0.17$). There is a fairly good correlation between the MLT from radiosonde data and HTI ($r = 0.641$, $p < 0.001$)

FIGURE 9 Annual and smoothed (with a 7-year running mean) HTI and both PDO trends and MEI trends for the study period. (a) Significant correlation are found between PDO and HTI ($r = 0.53$, $p < 0.001$), (—◆—) PDO index, (——) PDO smoothed, (—■—) HTI, and (——) HTI smoothed and (b) there is a positive correlation between MEI and HTI ($r = 0.34$, $p < 0.001$), (—◆—) MEI index, (——) MEI smoothed, (—■—) HTI, and (——) HTI smoothed [Colour figure can be viewed at wileyonlinelibrary.com]

elevation trend. This result is similar to that of GDL for 1919–2006, that is, the long-term trends do not indicate warming enhancement with elevation. But in contrast to GDL, high-elevation trends are also not higher than low-elevation trends in recent decades (Table 3). We note, however, that the highest station in Hawai'i (MLO) has been rapidly warming much faster (0.19°C/decade) than the high-elevation average (0.12°C/decade, $p < 0.001$) for the 1955–2016 time period. This suggests that the selected elevation range is too wide to properly see enhanced high-elevation warming. Indeed, an analysis of trends in air temperature lapse rates in Hawai'i (Kagawa-Viviani and Giambelluca, in review) suggests that air temperature trends in the elevation range of approximately 800–1,600 m have been very low or even negative during the past 50 years. Thus, if enhanced warming is occurring at the high-elevations, it is being cancelled by flat or negative trends in the lower part of "high-elevation" network used in our analysis. However, it also might be an artefact of the noisy signal produced by the small sample of high-elevation stations. While a higher limit would suffer greater uncertainty due to an even smaller sample of stations, it might better capture the elevation effect. Because it infers a more stable atmosphere, faster warming at high-elevations is consistent with the observed drier conditions during the past several decades in Hawaii (Frazier and Giambelluca, 2017). Greater scrutiny of elevation-related differences in Hawaii's air temperature trends is ongoing. In a separate study, Kagawa-Viviani and Giambelluca (*in review*) focus specifically on the spatial patterns of temperature change in Hawai'i.
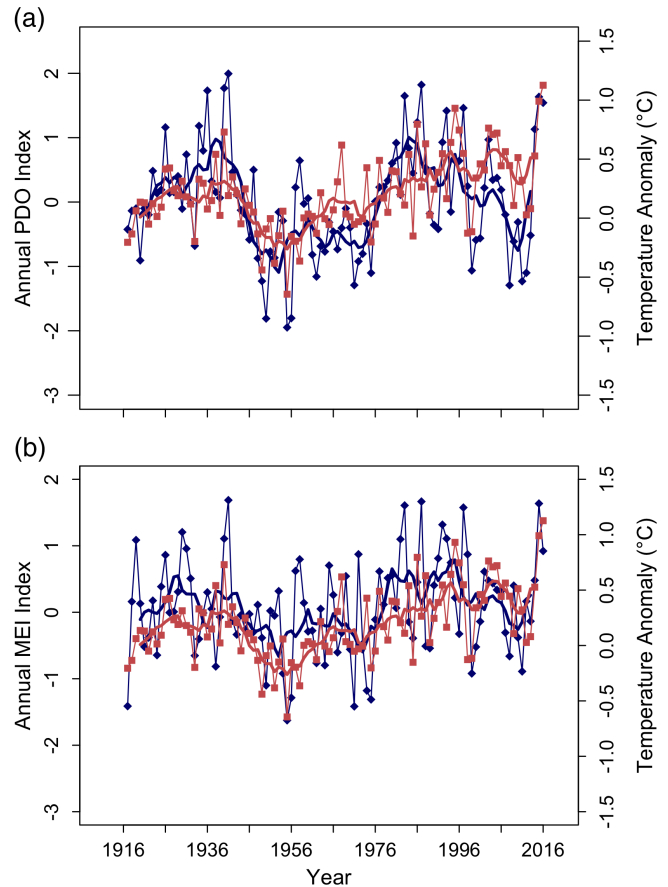
To gain more insight into the possible systematic temperature change for high-elevation tropical island sites, we compared temperature change at MLO (3,397 m), Hawai'i and the Mt. Izaña Observatory (2,373 m), Tenerife, Canary Islands, Spain. Mt. Izaña Observatory is the only high-elevation subtropical island site other than MLO with a long surface air temperature record, as far as we know. At these two stations, which differ in elevation by nearly 1,000 m, but are both located above the typical local trade wind inversion (TWI) height, the warming rates are virtually identical and quite high (0.19°C/decade, $p < 0.001$) for the period of overlapping records (1955–2016; Figure 12). While a sample of only two stations is not adequate to make sweeping generalizations, the rapid warming observed at these two sites suggests that they are affected in a similar way by ongoing large-scale climate warming. Furthermore, they are similarly located latitudinally, in the descending branch of the northern Hadley cell, albeit in different oceans, implying that the ongoing warming of the layer above the TWI might be systematic and widespread. It also indicates that the real
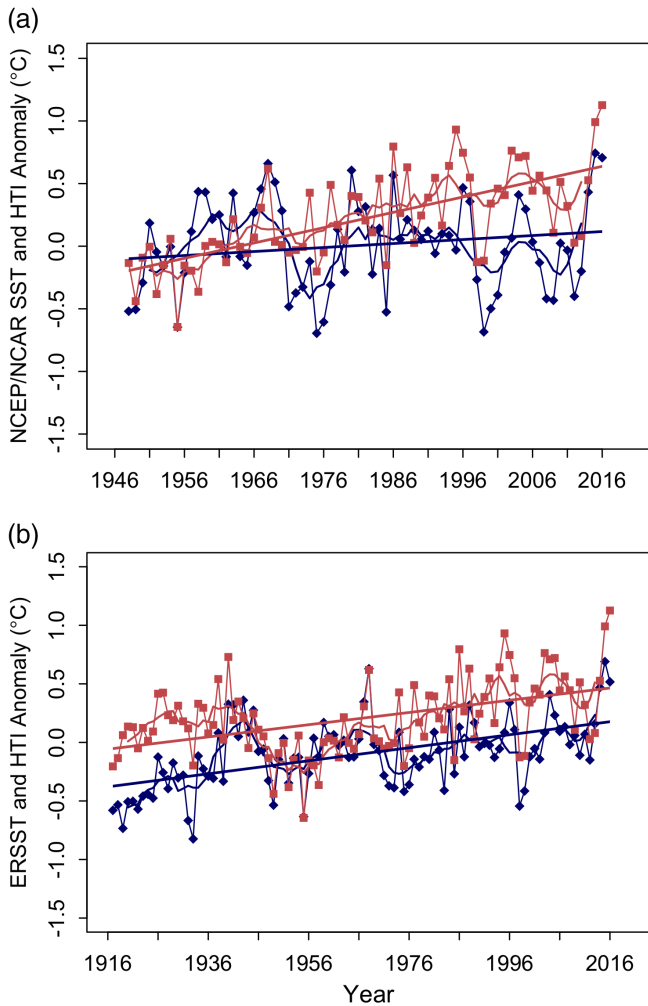
(a)

(b)

FIGURE 10 (a) SST anomaly for 16–24°N, 160–140°W using NCEP/NCAR reanalysis data in comparison with HTI for the 67-year period (1948–2016). SST trend is 0.032°C/decade (not significant, $p = 0.4$), and the warming trend of 0.122°C/decade for HTI between 1948 and 2016 ($p < 0.001$). There is positive correlation between HTI and SST ($r = 0.53$, $p < 0.001$). (—◆—) SST, (——) SST smoothed, (——) SST, linear trend: 1948–2016: 0.032°C/decade, (—■—) HTI, (——) HTI smoothed, (——) HTI, linear trend: 1948–2016: 0.122°C/decade. (b) ERSST v5 for 15–30°N, 170–140°W in comparison with HTI over the 100-year (1917–2016) record resulted in a warming trend of 0.052°C/decade ($p < 0.001$) and strong correlation between the two variables ($r = 65$, $p < 0.001$). (—◆—) ERSST, (——) ERSST smoothed, (——) ERSST, linear trend: 1917–2016: 0.056°C/decade, (—■—) HTI, (——) HTI smoothed, (——) HTI, linear trend: 1917–2016: 0.052°C/decade [Colour figure can be viewed at wileyonlinelibrary.com]

(a)

(b)

FIGURE 11 (a) HTI (base period 1917–2000), PDO and GLOTI time series (base period 1901–2000) comparison for the 1917–2016 time period. The GLOTI trend is 0.098°C/decade for the 100-year period. (■) HTI, linear trend: 1917–2016: 0.052°C/decade, (■) GLOTI, linear trend: 1917–2016: 0.098°C/decade, (– – –) HTI 20-year running mean, (– – –) GLOTI 20-year running mean, (– – –) PDO LOWEES-smoothed. (b) HTI (base period 1917–2000), PDO and GOTI time series (base period 1901–2000) comparison for the 1917–2016 time period. The global ocean trend is 0.081°C/decade for the 100-year period. (■) HTI, linear trend: 1917–2016: 0.052°C/decade, (■) GOTI, linear trend: 1917–2016: 0.081°C/decade, (– – –) HTI 20-year running mean, (– – –) GLOTI 20-year running mean, (– – –) PDO LOWEES-smoothed [Colour figure can be viewed at wileyonlinelibrary.com]

break in lowland/highland warming rates is not at 800 m, but rather near or above the inversion level, which is at a much higher altitude – around 2,000–2,300 m in Hawai'i (Longman *et al.,* 2015) and around 1,500 m in the Canary Islands (Sanroma *et al.,* 2010; Martín *et al.,* 2012).

Although rapid warming in the 800 m and above layer found by GDL has apparently not persisted based on the extended HTI, enhanced warming at the highest elevations (MLO) in Hawai'i comports with the abundant evidence of elevation dependent warming in mountains throughout the
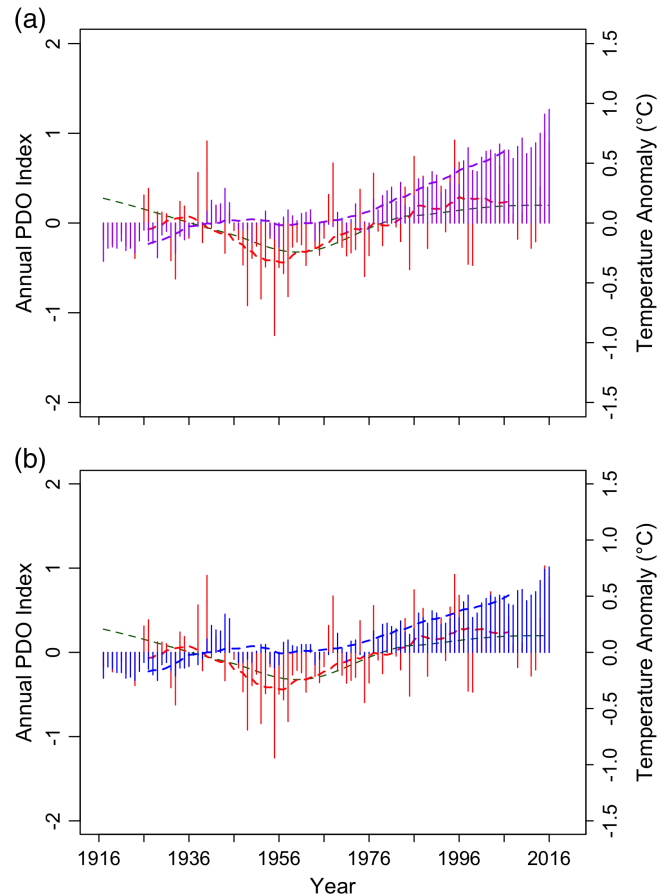
world (Pepin *et al.,* 2015). While several possible mechanisms have been identified (Rangwala and Miller, 2012; Pepin *et al.,* 2015), none point specifically to the zone above the TWI. We note that, areas above the TWI are warmer than they would be without the TWI. Hence, a more persistent TWI would enhance warming above the mean TWI level. Subsiding air in the descending branch of the regional Hadley circulation, which maintains the TWI, influences both Hawai'i and the Canary Islands. Longman *et al.* (2015) found consistent increases in the intensity and persistence of the TWI over the 1973–2013 period and found a good correlation between the TWI frequency of occurrence and the strength of Hadley cell subsidence in Hawai'i. Should the apparent uptick in Hadley cell overturning and consequent increase in TWI frequency of occurrence prove to be linked
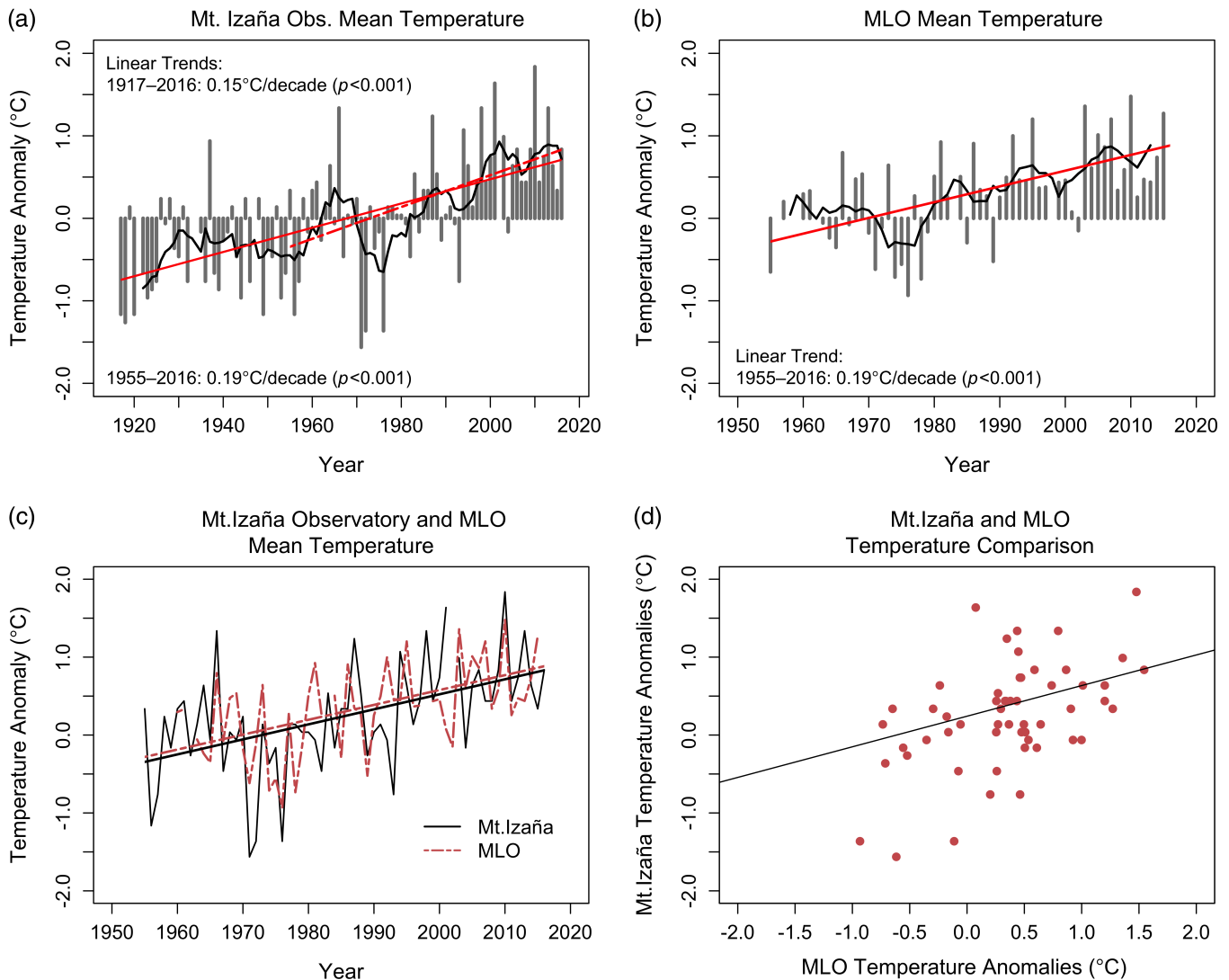
FIGURE 12 (a) and (b) annual mean surface temperature anomalies (grey bars), 7-year running means (black curve) and trends (red lines) at Mt. Izaña (2,373 m), Canary Islands, Spain, and Mauna Loa Observatory (MLO; 3,397 m), Hawai'i island, relative to a 1961–1990 baseline period. (a) Mt. Izaña has a significant warming rate of 0.15°C/decade (solid red line) for the century ($p < 0.001$; 1917–2016), and a significant trend of 0.19°C/decade ($p < 0.001$; dashed red line) over the recent 62-year period (1955–2016). (b) MLO also has a warming rate of 0.19°C/decade ($p < 0.001$; solid red line) over the 1955–2016 period. (c) Comparison of annual mean surface temperature anomalies on Mt. Izaña and MLO. (d) Scatterplot of MLO vs. Mt. Izaña annual temperature time series during 1955–2016 ($r = 0.51$, $p < 0.001$) [Colour figure can be viewed at wileyonlinelibrary.com]

to global climate change, as suggested by downscaled climate projections for Hawai'i (Lauer *et al.*, 2013), rapid warming at high-elevations in Hawai'i is likely to continue.

As the global climate warms, Hawai'i is likely to see increasing atmospheric stability, due in part to a more persistent TWI (Cao *et al.*, 2007; Lauer *et al.*, 2013). In the Canary Islands, an intensification of the trade wind circulation in the northern windward slopes of the Canary Islands is expected with increases in wet and humid air below the inversion, but above the inversion, with the strengthening of the Hadley cell, the air is dry and clear (Sanroma *et al.*, 2010). Although mean temperature and precipitation are known to be strongly modulated by ENSO in Hawai'i, interannual to decadal drivers of climatic variability in Canary Islands are generally different. Nonetheless, the similarity in the observed rate of

warming in response to global climate change at these two widely separated sites is striking.

T_{min} in Hawai'i has increased over the long-term period, while T_{max} has not increased significantly. These results translate to a considerable drop in the DTR. Vose *et al.* (2005) found a global trend in DTR of -0.066°C/decade over land areas between 1950 and 2004 as a result of increased rapid T_{min} rise. Malamud *et al.* (2011) showed that greater increases in T_{min} compared with T_{max} at Mauna Loa Observatory had caused DTR to decrease by -0.50°C/decade over the period 1977–2006. Martín *et al.* (2012) also found greater night time warming for high-elevation areas of Tenerife.

Throughout the 100-year record, temperature anomalies have experienced periods of both positive and negative

trends. However, the long-term trend is positive, with new record highs in recent years. Based on the HTI, 2015 and 2016, which were influenced by one of the strongest El Niño events on record, were the warmest years throughout the 100-year study period at 0.788 and 0.924°C above the 100-year mean, respectively. The extreme positive temperature anomaly associated with the 2015–2016 event reached 1.5°C during July–October 2015 (Zhu and Li, 2017).

5 | CONCLUSION

We refined a previous HTI index and extended the record by 12 years from the earlier reported 88-year time series (1919–2006, GDL 2008) to a 100-year trend series (1917–2016). To minimize the effects of discontinuous station data records, an improved HTI was developed. We compared the station-based results with other datasets (e.g., radiosonde and Reanalysis data). The various resulting temperature series were consistent with the HTI results, both well correlated and exhibiting similar trends. The long-term trends for T_{mean}, T_{min}, or T_{max} anomalies for state-wide, low-, and high-elevation stations were assessed. T_{mean} and T_{min} for the 100-year study period state-wide showed significant rates of warming (0.052°C/decade and 0.072°C/decade, respectively). T_{mean} trends by elevation showed higher rates of warming at low-elevations (0.056°C/decade) compared to the high-elevation stations (0.047°C/decade) over the last century. However, much higher rates of warming are evident above the TWI at Hawaii's highest elevation station, MLO, and at Mt. Izaña Observatory in the Canary Islands. The regional effects of the global warming slowdown beginning in the early 2000s coinciding with a phase change in the PDO continue into the additional recent years added to the HTI record. However, rapid warming appears to have resumed in Hawai'i early in 2014.

ORCID

Marie M. McKenzie https://orcid.org/0000-0002-9365-4286

REFERENCES

Cao, G., Giambelluca, T.W., Stevens, D.E. and Schroeder, T.A. (2007) Inversion variability in the Hawaiian trade wind regime. *Journal of Climate*, 20, 1145–1160. https://doi.org/10.1175/JCLI4033.1.

Dai, A., Fyfe, J.C., Xie, S.-P. and Dai, X. (2015) Decadal modulation of global surface temperature by internal climate variability. *Nature Climate Change*, 5, 555–559.

Diaz, H.F. and Giambelluca, T.W. (2012) Changes in atmospheric circulation patterns associated with high and low rainfall regimes in the Hawaiian islands region on multiple time scales. *Global and Planetary Change*, 98-99, 97–108.

Diaz, H.F., Giambelluca, T.W. and Eischeid, J.K. (2011) Changes in the vertical profiles of mean temperature and humidity in the Hawaiian islands. *Global and Planetary Change*, 77(1–2), 21–25. https://doi.org/10.1016/j.gloplacha.2011.02.007.

Diaz, H.F., Bradley, R.S. and Ning, L. (2014) Climatic changes in mountain regions of the American cordillera and the tropics. *Arctic, Antarctic, and Alpine Research*, 46, 735–743. https://doi.org/10.1657/1938-4246-46.4.735.

Elliott, W.P., Gaffen, D.J., Angell, J.K. and Kahl, J.D.W. (1994) The effect of moisture on layer thicknesses used to monitor global temperatures. *Journal of Climate*, 7(2), 304–308. https://doi.org/10.1175/1520-0442(1994)007<0304:TEOMOL>2.0.CO;2.

Frazier, A.G. and Giambelluca, T.W. (2017) Spatial trend analysis of Hawaiian rainfall from 1920 to 2012. *International Journal of Climatology*, 37, 2522–2531. https://doi.org/10.1002/joc.4862.

Frazier, A.G., Elison Timm, O., Giambelluca, T.W. and Diaz, H.F. (2018) The influence of ENSO, PDO and PNA on secular rainfall variations in Hawai'i. *Climate Dynamics*, 51, 2127–2140. https://doi.org/10.1007/s00382-017-4003-4.

Giambelluca, T.W., Diaz, H.F. and Luke, M.S.A. (2008) Secular temperature changes in Hawai'i. *Geophysical Research Letters*, 35(12), L12702. https://doi.org/10.1029/2008GL034377.

Huang, B., Thorne, P.W., Banzon, V.F., Boyer, T., Chepurin, G., Lawrimore, J.H., Menne, M.J., Smith, T.M., Vose, R.S. and Zhang, H.-M. (2017) NOAA extended reconstructed sea surface temperature (ERSST), Version 5. [SST/-Skin T, 1916–2016]. NOAA, National Centers for Environmental Information. https://doi.org/10.7289/V5T72FNM accessed August 14, 2018.

Huber, U.M., Bugmann, H.K. and Reasoner, M.A. (2006) *Global change and mountain regions: an overview of current knowledge*. Dordrecht, The Netherlands: Springer.

Juvik, S.P. and Juvik, J.O. (1998) *Atlas of Hawai'i*, 3rd edition. Honolulu, Hawai'i: University of Hawai'i Press.

Keener, V.W., Marra, J.J., Finucane, M.L., Spooner, D. and Smith, M.H. (Eds.). (2012) *Climate change and pacific islands: indicators and impacts: Report for the 2012 Pacific Islands Regional climate assessment*. Washington, DC: Island Press.

Kistler, R., Collins, W., Saha, S., White, G., Woollen, J., Kalnay, E., et al. (2001) The NCEP-NCAR 50-year reanalysis: monthly means CD-ROM and documentation. *Bulletin of the American Meteorological Society*, 82(2), 247–267.

Lauer, A., Zhang, C., Elison-Timm, O., Wang, Y. and Hamilton, K. (2013) Downscaling of climate change in the Hawaii region using CMIP5 results: on the choice of the forcing fields. *Journal of Climate*, 26(24), 10006–10030. https://doi.org/10.1175/JCLI-D-13-00126.1.

L'Heureux, M.L., et al. (2017) Observing and predicting the 2015/16 El Niño. *Bulletin of the American Meteorological Society*, 98(7), 1363–1382. https://doi.org/10.1175/BAMS-D-16-0009.1.

Longman, R.J., Diaz, H.F. and Giambelluca, T.W. (2015) Sustained increases in lower-tropospheric subsidence over the central tropical North Pacific drive a decline in high-elevation rainfall in Hawaii. *Journal of Climate*, 28(22), 8743–8759. https://doi.org/10.1175/JCLI-D-15-0006.1.

Malamud, B.D., Turcotte, D.L. and Grimmond, C.S.B. (2011) Temperature trends at the Mauna Loa observatory. *Hawaii. Climate Past*, 7(3), 975–983. https://doi.org/10.5194/cp-7-975-2011.

Mantua, N.J. and Hare, S. (2002) Pacific-Decadal Oscillation (PDO). *Encyclopedia of global environmental change*, 1, 592–594.

Mantua, N.J., Hare, S.R., Zhang, Y., Wallace, J.M. and Francis, R.C. (1997) A Pacific Interdecadal climate oscillation with impacts on Salmon production. *Bulletin of the American Meteorological Society*, 78(6), 1069–1079. https://doi.org/10.1175/1520-0477(1997)078<1069:APICOW>2.0.CO;2.

Martín, J.L., Bethencourt, J. and Cuevas-Agulló, E. (2012) Assessment of global warming on the Island of Tenerife, Canary Islands (Spain). Trends in minimum, maximum and mean temperatures since 1944. *Climatic Change*, 114 (2), 343–355. https://doi.org/10.1007/s10584-012-0407-7.

National Centers for Environmental Information (NOAA), Climate at a Glance: U.S. Time Series, 2017, retrieved on February 16, 2017, from http://www.ncdc.noaa.gov/cag/

Pachauri, R.K., Allen, M.R., Barros, V.R., Broome, J., Cramer, W., Christ, R., et al. (2014) Climate Change 2014: Synthesis Report. In: Pachauri, R. and Meyer, L. (Eds.) *Contribution of Working Groups I, II and III to the Fifth Assessment Report of the Intergovernmental Panel on Climate Change*. Geneva, Switzerland: IPCC, p. 151. isbn:978–92–9169-143-2.

Pepin, N., Bradley, R.S., Diaz, H.F., Baraer, M., Caceres, E.B., Forsythe, N., Greenwood, G., et al. (2015) Elevation-dependent warming in mountain regions of the world. *Nature Climate Change*, 5, 424–430. https://doi.org/10.1038/NCLIMATE2563.

Pinheiro J, Bates D, DebRoy S, Sarkar D and R Core Team (2017). Nlme: linear and nonlinear mixed effects models. R package version 3.1-131, URL: https://CRAN.R-project.org/package=nlme.

R Core Team. (2014) *R: a language and environment for statistical computing*. Vienna, Austria: R Foundation for Statistical Computing URL http://www.R-project.org/.

Rangwala, I. and Miller, J.R. (2012) Climate change in mountains: a review of elevation-dependent warming and its possible causes. *Climatic Change*, 114, 527–547. https://doi.org/10.1007/s10584-012-0419-3.

Salinger, M.J. (2005) Climate variability and change: past, present and future — an overview. In: Salinger, J. , Sivakumar, M.V.K. and Motha, R.P. (Eds.) *Increasing climate variability and change: Reducing the vulnerability of agriculture and forestry*. Dordrecht: Springer Netherlands, pp. 9–29. https://doi.org/10.1007/1-4020-4166-7_3.

Sanroma, E., Palle, E. and Sanchez-Lorenzo, A. (2010) Long-term changes in insolation and temperatures at different altitudes. *Environmental Research Letters*, 5(2), 024006. https://doi.org/10.1088/1748-9326/5/2/024006.

Schneider, N. and Cornuelle, B.D. (2005) The forcing of the Pacific decadal oscillation. *Journal of Climate*, 18(21), 4355–4373. https://doi.org/10.1175/JCLI3527.1.

Toumi, R., Hartell, N. and Bignell, K. (1999) Mountain Station pressure as an indicator of climate change. *Geophysical Research Letters*, 26(12), 1751–1754. https://doi.org/10.1029/1999GL900351.

Vose, R.S., Easterling, D.R. and Gleason, B. (2005) Maximum and minimum temperature trends for the globe: an update through 2004. *Geophysical Research Letters*, 32(23), L23822. https://doi.org/10.1029/2005GL024379.

Wallace, J.M. and Hobbs, P.V. (1977) *Atmospheric science, an introductory survey*. New York: Academic Press.

Wolter, K. and Timlin, M.S. (1998) Measuring the strength of ENSO events: how does 1997/98 rank? *Weather*, 53(9), 315–324. https://doi.org/10.1002/j.1477-8696.1998.tb06408.x.

Zhang, Y., Wallace, J.M. and Battisti, D.S. (1997) ENSO-like Interdecadal Variability: 1900-93. *Journal of Climate*, 10(5), 1004–1020. https://doi.org/10.1175/1520-0442(1997)010<1004:ELIV>2.0.CO;2.

Zhu, Z. and Li, T. (2017) The record-breaking hot summer in 2015 over Hawaii and its physical causes. *Journal of Climate*, 30(11), 4253–4266. https://doi.org/10.1175/JCLI-D-16-0438.1.